Specific heat of single-crystal $PrMnO_3$

2005 J. Phys.: Condens. Matter 17 5869

(http://iopscience.iop.org/0953-8984/17/37/022)

INSTITUTE OF PHYSICS PUBLISHING JOURNAL OF PHYSICS: CONDENSED MATTER

J. Phys.: Condens. Matter **17** (2005) 5869–5879 doi:10.1088/0953-8984/17/37/022

Specific heat of single-crystal $PrMnO_3$

J G Cheng[1], Y Sui[1,2], X J Wang[1], Z G Liu[1], J P Miao[1], X Q Huang[1], Z Lü[1], Z N Qian[1] and W H Su[1,2,3]

[1] Center for Condensed Matter Science and Technology (CCMST), Department of Applied Physics, Harbin Institute of Technology, Harbin 150001, People's Republic of China
[2] International Center for Materials Physics, Academia Sinica, Shenyang 110015, People's Republic of China

E-mail: suiyu@hit.edu.cn

Received 7 June 2005, in final form 12 August 2005
Published 2 September 2005
Online at stacks.iop.org/JPhysCM/17/5869

Abstract

The specific heat of single-crystal $PrMnO_3$ was investigated from 2 to 200 K under different magnetic fields up to 8 T. A Schottky-like anomaly observed at low temperature was gradually shifted to higher temperatures by magnetic fields. The first four singlets of the Pr^{3+} $^3H_4$ ground multiplet in $PrMnO_3$ are given for the first time by fitting the specific heat of Pr^{3+} ions below 40 K under zero field. By analysing the field dependence of the first singlet of Pr^{3+} ions, the Pr–Mn exchange field is found to be negligible, which is consistent with the magnetic anisotropy of Pr^{3+} ions revealed in the magnetic measurement. At T_N, the cooperative antiferromagnetic ordering of Mn^{3+} spins shows up as λ-shaped anomaly, which is lowered and broadened in magnetic fields. The magnetic entropy near T_N is estimated by subtracting the contributions to specific heat from Pr^{3+} ions and lattice vibrations. It was found that the fraction of entropy above T_N in the total entropy increases with the fields due to the enhancement of spin fluctuations by magnetic field.

1. Introduction

In recent years, the mixed-valent perovskite manganites $R_{1-x}A_xMnO_3$ (R and A being a trivalent rare-earth and a divalent alkaline-earth ion, respectively) have attracted extensive investigations due to the presence of fascinating magnetic and transport properties, such as the colossal magnetoresistance, charge/orbital/spin ordering and phase separation [1]. Complementary to, and to some extent independent of, measurements of magnetic and transport properties, the specific heat measurements have been shown repeatedly to be a useful technique to detect information about the ground states and discover new phenomena [2–5]. For example, the enhanced electron density of states over free-electron and band-structure calculations observed by Hamilton *et al* in the low-temperature specific heat of $La_{0.67}Ba_{0.33}MnO_3$ and

[3] Author to whom any correspondence should be addressed.

$La_{0.8}Ca_{0.2}MnO_3$ indicated the importance of electron–lattice coupling in these manganites [2]. The systematic study of specific heat of the $Pr_{0.6}(Ca_{1-x}Sr_x)_{0.4}MnO_3$ ($0 \leqslant x \leqslant 1$) system enabled Lees *et al* to observe the gradual change of the ground state from metallic ferromagnet for $x \geqslant 0.25$ to the antiferromagnetic charge-ordered insulator at the end $x = 0$ [3]. In addition, a Schottky-like specific heat anomaly at low temperature was found by Gordon *et al* in $Nd_{0.67}Sr_{0.33}MnO_3$ and attributed to the Nd^{3+} ion ordering due to Nd–Mn exchange field [4]. In a latter work, López *et al* observed a similar Schottky-like anomaly in a series of charge-ordered manganites $R_{0.5}A_{0.5}MnO_3$ (R = Nd, Sm, Dy, Ho; A = Ca, Sr) containing rare-earth ions with magnetic moment [5]. But it was found that the Schottky-like anomalies in that study cannot be fitted with either a two-level or a distribution of two-level Schottky anomaly [5]; it appears that the excess specific heat of nonmagnetic origin associated with charge ordering found by Smolyaninova *et al* [6] might complicate the analysis of the low-temperature specific heat in these charge-ordered manganites. Although it has been attempted to correlate the Schottky-like anomaly with the magnetic rare-earth ions, the absence of any Schottky-like anomaly in the low-temperature specific heat of mixed-valent manganites containing Pr^{3+} ions with the same magnetic moment as Nd^{3+} ions, such as $Pr_{0.63}Ca_{0.37}MnO_3$ [7, 8], makes such correlation inaccurate. However, recently the specific heat of $PrMnO_3$ exhibited a Schottky-like anomaly at low temperature due to the low-lying quasidoublet split by the crystal electric field (CEF) [9], which is different from the mixed-valent manganites containing Pr^{3+} ions. Such discrepancy has not been clarified so far. Thus, it will be easier to study the single-valent $PrMnO_3$ for clarifying the contribution of rare-earth ions to the low-temperature specific heat. Although the Schottky-like anomaly in specific heat of $PrMnO_3$ has been shown in [9], there is no detailed analysis concerning the contribution from Pr^{3+} ions, and the field-independent specific heat in that study is in contrast with our present field-induced shift of Schottky-like anomaly in the specific heat measurement.

It has been shown previously that the field-induced shift of Schottky-like specific heat anomaly in $NdMnO_3$ can be correlated with the ground state of Nd^{3+} ions [10]. The ground state of Nd^{3+} ions, $^4I_{9/2}$, is split into five Kramers doublets by CEF according to the Kramers theorem [11]. It is the splitting of the first Kramers doublet due to Nd–Mn exchange field that causes the Schottky-like anomaly in the low-temperature specific heat. The magnetic field plays a role of additive magnetic field on the Nd–Mn exchange field, leading to the linear field dependence of the splitting of the first doublet [10]. Correspondingly, the contribution of Nd^{3+} moments at low temperature due to the polarization by the Nd–Mn exchange field along the *c* axis has to be considered in order to explain the high magnetic ac susceptibility and spontaneous ferromagnetic component along the *c* axis in addition to the canted type-A antiferromagnetic (A-AF) structure of Mn spins [9]. Thus, through analysing the field dependence of the Schottky-like anomaly in $PrMnO_3$ observed by us, we can shed light on the ground state of Pr^{3+} ions which is found to have rather different contribution to low-temperature magnetic properties compared with the Nd^{3+} ions in $NdMnO_3$ [9, 12].

In this study, the specific heats of single-crystal $PrMnO_3$ under different magnetic fields up to 8 T were investigated in detail. The first four singlets of the Pr^{3+} $^3H_4$ ground multiplet were determined by fitting the low-temperature specific heat under zero field, and the anisotropy ground state of Pr^{3+} ions was discussed in connection with the field dependence of the Schottky-like anomaly. In addition, the field dependence of the λ-shaped anomaly at T_N was shown to correlate with the enhanced spin fluctuations of Mn^{3+} sub-lattice by magnetic field.

2. Experiments

The single-crystal $PrMnO_3$ sample in our experiment has been grown in an argon atmosphere from ceramic bars in an infrared-heating image furnace and has been used in a number of

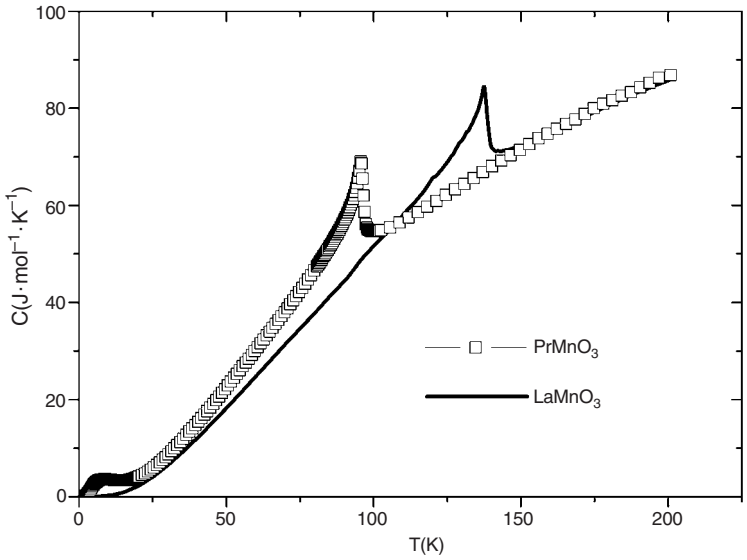

Figure 1. Specific heat of single-crystal $LaMnO_3$ and $PrMnO_3$ under zero field from 2 to 200 K.

previous experiments [13, 14]. The sample is single phase to x-ray powder diffraction. The oxygen stoichiometry has been checked carefully to within 0.1% by measurement of thermoelectric power as shown in [13]. The specific heat measurements were carried out by means of PPMS (Quantum Design) using the two-τ relaxation method, at temperatures from 2 to 200 K and under magnetic fields up to 8 T. The background from the sample holder and the Apiezon N grease used to paste the sample on the platform was recorded in a first run and was subtracted from the total specific heat. The specific heat of single-crystal $LaMnO_3$ sample under zero field was also measured in order to subtract the background specific heat contributions from lattice vibrations and spin-wave excitations in $PrMnO_3$.

3. Results and discussion

Figure 1 shows the specific heats of single-crystal $LaMnO_3$ and $PrMnO_3$ under zero field from 2 to 200 K. Corresponding to the A-AF ordering of the Mn^{3+} spin sub-lattice in these compounds, a similar λ-shaped anomaly is observed at $T_N = 136$ and 96 K for $LaMnO_3$ and $PrMnO_3$, respectively, which are in agreement with those reported in the literature [9, 12]. The decrease of T_N is caused by the increase of the bending of the $(180° - \varphi)$ Mn–O–Mn bond angle due to the decrease of ion size from La^{3+} to Pr^{3+} [14]. Furthermore, a significant Schottky-like anomaly is clearly observed at low temperatures below 20 K in the $PrMnO_3$ sample, while the specific heat of $LaMnO_3$ varies like the common solids at low temperature. By subtracting the specific heat of isostructural nonmagnetic $LaGaO_3$ from $NdCrO_3$, Bartolomé *et al* have been able to separate and quantify the different magnetic contributions from the Nd^{3+} and Cr^{3+} sub-lattices due to the rather high $T_N = 219$ K [15]. In that study the CEF energy levels derived from the fitting of specific heat of Nd^{3+} ions are in agreement with the available neutron-scattering spectral lines [15]. But the relatively low $T_N = 96$ K as well as the ninefold ground multiplet in our case makes the above-mentioned treatment infeasible. Thus, the specific heat of $LaMnO_3$ with the same crystalline and magnetic structures as $PrMnO_3$ was subtracted below 40 K in order to obtain the magnetic specific heat of Pr^{3+} ions, denoted as

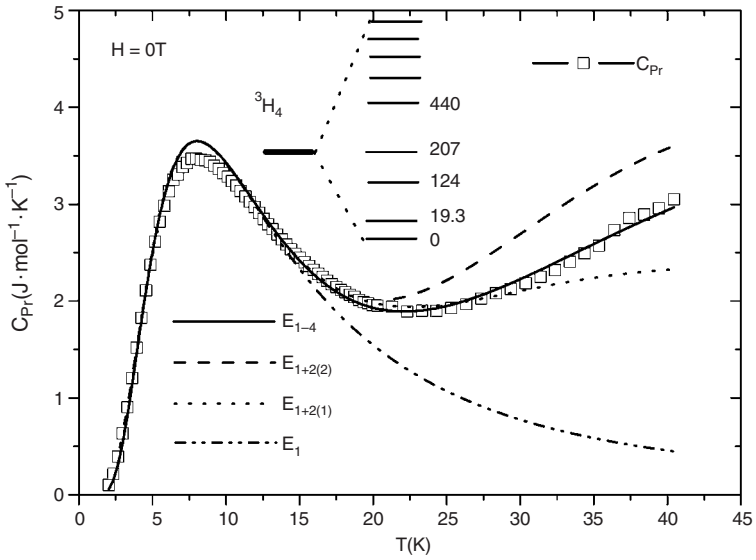

Figure 2. Specific heat of Pr^{3+} ions below 40 K under zero field calculated by subtracting the specific heat of $LaMnO_3$ from $PrMnO_3$. The dash–dot–dot line represents the best fitting of data below 10 K by considering the contribution from the first singlet E_1. The dotted and dashed lines represent the best fitting of data below 20 K by considering the contribution from the first and second singlet $E_{1+2(1)}$ and the first singlet and second doublet $E_{1+2(2)}$. The solid line represents the best fitting of data up to 40 K by taking into account contributions from the first four singlets in the Pr^{3+} $^3H_4$ ground multiplet E_{1-4}. The first four CEF levels derived from the best fit are shown in the scheme.

C_{Pr} and shown in figure 2. The difference of lattice vibrations due to the slight difference of atom mass between La and Pr is negligible compared with the large contribution of Pr^{3+} ions. In addition, the upper limit is chosen to be 40 K, much lower than the T_N of both $LaMnO_3$ and $PrMnO_3$, in order to avoid their critical regions and make a good approximation of their spin-wave excitations.

The ground state of the Pr^{3+} ion is $^3H_4$, where H stands for an orbital angular momentum $L = 5$, the super-prefix specifies the total spin as $2S + 1$ and the subscript the total angular momentum J. The ninefold degeneracy of the ground-state J multiplet of the Pr^{3+} ions in $PrMnO_3$ will be lifted by the CEF, which will lead to the Schottky-like anomaly due to the thermal population of electrons in these energy levels. (The possible split due to Pr–Mn exchange interaction will be shown to be nearly negligible later on.) Thus, the separation of C_{Pr} from total specific heat enables us to investigate the CEF levels of Pr^{3+} ions in $PrMnO_3$, which has not been investigated so far to our knowledge. In the following, we will denote the nth CEF level as E_n ($0 \leqslant n \leqslant 8$). The CEF levels of the Pr^{3+} ions in the isostructural perovskites $PrNiO_3$ and $PrGaO_3$ have been investigated by inelastic neutron scattering in [16] and [17]. In $PrNiO_3$, five inelastic lines at 74, 174, 235, 440, and 696 K, respectively, are observed and ascribed to the first four and the seventh CEF levels of Pr^{3+} ions [16]. It should be noted that the second level E_2 is doubly degenerate. In $PrGaO_3$, six inelastic lines, at 59, 186, 249, 440, 777, and 997 K, respectively, are evidenced and ascribed to the first six CEF levels of Pr^{3+} ions, in which the fifth level is also doubly degenerate [17]. Most of the energy levels below 440 K in these two compounds are comparable, with the exception that the E_2 is doubly degenerate (denoted by $E_{2(2)}$) in $PrNiO_3$ while a singlet ($E_{2(1)}$) in $PrGaO_3$. In the following analysis we will show that the E_2 of the Pr^{3+} ion in $PrMnO_3$ is a singlet as in $PrGaO_3$.

The C_{Pr} under zero field below 40 K is shown in figure 2. From the CEF levels of $PrNiO_3$ and $PrGaO_3$, the E_2 (whether $E_{2(2)}$ or $E_{2(1)}$) is so high that the rounded maximum at $T_S \approx 8$ K is predominantly due to the two-level Schottky anomaly caused by the E_0 and E_1. Thus, the data below 10 K (just above T_S) can be fitted by using the function of the two-level Schottky anomaly $C(E_1) = E_1^2/[T^2 \cosh(E_1/2k_BT)]^2$ [18] and the fitted curve is shown in figure 2 as the dash–dot–dot line. It was found that the data can be fitted well below 13 K except for the slight difference near the maximum, which cannot be eliminated by adjusting the fitting parameter E_1 and might arise from the excess subtraction of background. Above 13 K, we must consider the contributions from higher levels. Then, we extrapolate the fit to 20 K and check the possible configuration of E_2. It was found that although the data below 20 K can be fitted well by considering the contributions from $E_{1+2(1)}$ or $E_{1+2(2)}$, the curve of $E_{1+2(2)}$ is always above the data of C_{Pr} above 20 K, suggesting an improper situation for Pr^{3+} ions in $PrMnO_3$. Instead the curve of $E_{1+2(1)}$ can represent well the C_{Pr} to almost 30 K, which confirms that the E_2 of Pr^{3+} ions in $PrMnO_3$ is a singlet as in $PrGaO_3$. Finally, we extend the fitting range up to 40 K and take into account the contributions from the third and fourth singlets (E_3 and E_4). As seen from the CEF levels of $PrNiO_3$ and $PrGaO_3$, the E_4 (440 K) is same for them and is actually so high that the data below 40 K are not sensitive to the change of E_4. Thus, we keep the $E_4 = 440$ K as constant in our following fitting procedures and leave E_1 to E_3 as new parameters in order to fit the data below 40 K. It can be seen that the solid line of E_{1-4} in figure 2 can describe well the data of C_{Pr} below 40 K. The first four CEF levels derived from the above fitting procedure are shown in figure 2. It was found that the CEF levels of Pr^{3+} ions in $PrMnO_3$ are lower than those in $PrNiO_3$ and $PrGaO_3$; in particular, the E_1 of 19.28 ± 0.20 K is much lower than 74 and 59 K. Although all three compounds containing Pr^{3+} ions are crystallized in the orthorhombic perovskite-type structure and the Pr^{3+} ions occupy the 4c site with the site symmetry C_s-m [16, 17], the E_1 is quite different from each other. As already stated, the significant maximum at $T_S \approx 8$ K is predominantly caused by the splitting of E_1 from E_0. For a two-level Schottky function, the peak temperature in the specific heat can be simply related to the energy splitting of the two levels (Δ) by $\Delta = T_S/0.418$. Thus, the peak temperatures of the two-level Schottky anomaly in the specific heat of $PrNiO_3$ and $PrGaO_3$ will be 31 and 25 K, respectively, but such a Schottky-like anomaly might be indistinguishable due to the dominant contribution from lattice vibrations. The above discussion might be applied to the mixed-valent perovskite-type manganites containing Pr^{3+} ions [3, 7, 8], such as $Pr_{0.63}Ca_{0.37}MnO_3$; i.e. the E_1 in these compounds might be much higher than that of $PrMnO_3$ so that the possible Schottky-like anomaly cannot be distinguished in the specific heat measurement. Thus, it appears that the different CEF environments in the mixed- and single-valent manganites containing Pr^{3+} ions should be responsible for the discrepancy of the absence of any Schottky-like anomaly in the former and the presence in the latter as mentioned in the introduction.

The C_{Pr} curves under different magnetic fields up to 8 T are shown in figure 3. It was found that the Schottky-like anomaly is gradually shifted to higher temperatures by magnetic fields. Fitting procedures similar to that for C_{Pr} under zero field are also performed to fit the C_{Pr} under magnetic fields by taking into account the contributions from the first four singlets and keeping E_4 as constant. It can be seen that the fitting curves can excellently represent the specific heat data in figure 3. The CEF levels under magnetic fields derived from the best fits as well as their standard deviation are given in table 1. It was found that with increasing magnetic fields E_1 and E_2 increase, but E_3 changes little within the range of fitting error. It has been shown that the magnetic field reduces the Debye temperature but increases the A-AF spin-wave stiffness in $NdMnO_3$ [10]. Thus, we think that it is suitable to estimate the C_{Pr} under magnetic fields by subtracting the specific heat of $LaMnO_3$ under zero field below 20 K. The increasing of E_1 and E_2 is consistent with the above approximation.

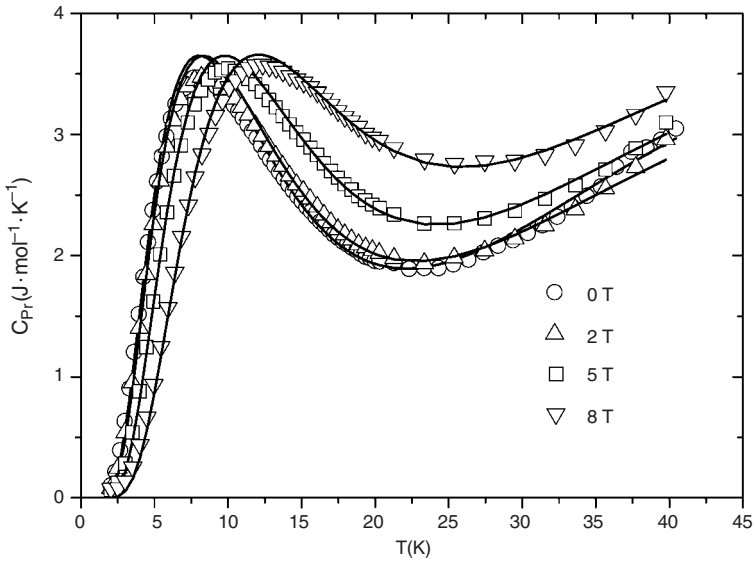

Figure 3. The C_{Pr} below 40 K under different magnetic fields up to 8 T and their best fits by taking into account the first four singlets in the Pr^{3+} $^3H_4$ ground multiplet.

Table 1. The fit parameters obtained from the best fits of C_{Pr} under different magnetic fields. SD represents the standard deviation of the best fit.

H (T)	E_1 (K)	E_2 (K)	E_3 (K)	E_4 (K)	$(SD)^2$
0	19.28(0.20)	124.6(4.2)	207.5(10.2)	440	0.5566
2	20.02(0.23)	129.8(5.2)	225.8(10.5)	440	0.2993
5	23.39(0.21)	134.3(4.3)	216.3(12.1)	440	0.1764
8	28.75(0.27)	140.0(4.9)	215.4(13.1)	440	0.1917

Even though some errors will be introduced in fitting C_{Pr} data under magnetic fields by subtracting the specific heat of $LaMnO_3$ under zero field, the E_1 is least influenced because it is determined mainly from the maximum temperature in the specific heat curves. Thus, the field dependence of E_1, shown in figure 4, can provide us with important information about the ground state of Pr^{3+} ions. It was found that E_1 increases nonlinearly with increasing magnetic fields, unlike the linear increase of the splitting of the Nd^{3+} first doublet in $NdMnO_3$ [10]. In $PrMnO_3$, the Schottky-like specific heat anomaly arises mainly from the low-lying quasidoublet, E_1 and E_0, split by CEF, if we suppose that the Pr–Mn exchange interaction can also contribute to the split of E_1 and E_0, and then the field dependence of the E_1 can be described by [9]

$$E_1(H) = \{E_{1CEF}^2 + [2\mu_{eff}(H_{ex} + H)]^2\}^{1/2} \quad (1)$$

where the E_{1CEF} is the splitting by CEF, μ_{eff} is the effective magnetic moment per Pr^{3+} ion, H_{ex} is the Pr–Mn exchange field at Pr^{3+} sites and H is the magnetic field. When we try to fit the field dependence of E_1, H_{ex} has to be kept below 0.001 mT in order to obtain a reasonable fit. In fact, we can fit E_1 excellently without considering the contribution of H_{ex}. Thus, the $E_{1CEF} = 19.28 \pm 0.19$ K and $\mu_{eff} = 1.33 \pm 0.01$ μ_B can be obtained through fitting E_1 by using equation (1) with $H_{ex} = 0$; the excellent fitting curve is shown in figure 4 as the solid line. The $E_{1CEF} = 19.28$ K is quite consistent with those of 18.7 K obtained

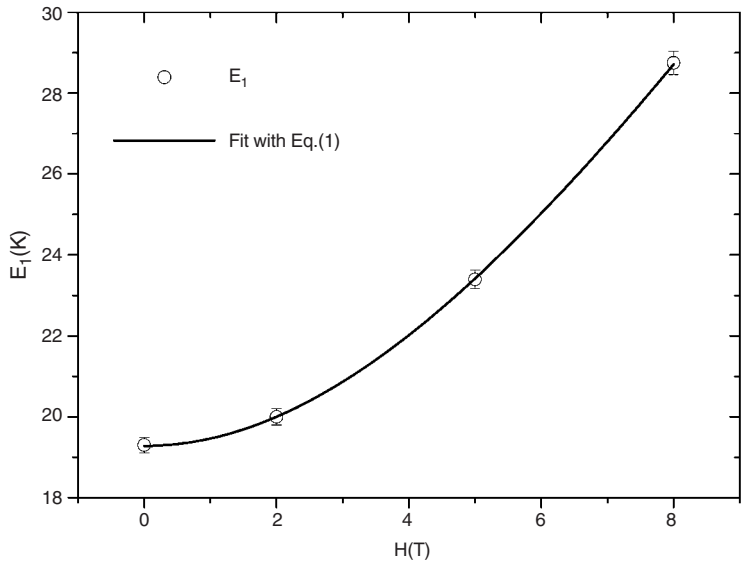

Figure 4. Field dependence of E_1 of Pr^{3+} ions in $PrMnO_3$ and its best fit by using equation (1) in the text.

from magnetization and submillimetre transition spectrum measurements [9, 12]. The smaller $\mu_{\text{eff}} = 1.33\ \mu_B$ compared with $\mu_{\perp C} = 2.1\ \mu_B$ from magnetization measurement [9, 12] should arise from the average effect of applied field on the Pr^{3+} ions. Furthermore, the negligible H_{ex} is in good agreement with the anisotropy behaviour of Pr^{3+} ions and weak spontaneous ferromagnetic moment along the c axis revealed from magnetic ac susceptibility and magnetization measurements [9, 12]. In $PrMnO_3$ the ac susceptibility towards low temperatures reveals a strong increase parallel to the ab plane, but remains almost constant along the c direction, similar to that of $LaMnO_3$, implying that the moments of the Pr ions are oriented within the ab plane. The spontaneous ferromagnetic moment along the c axis in $PrMnO_3$ is about 0.09 μ_B, comparable with that of $LaMnO_3$, but is smaller by a factor of 20 than that of $NdMnO_3$ [9, 12]. According to the canted A-AF structure of the Mn^{3+} spin sub-lattice A_xF_z, antiferromagnetically coupled Mn layers will give rise to a zero magnetic field at Pr^{3+} sites with respect to the x direction, where the moments of Pr^{3+} ions lie. While the ferromagnetic component of Mn spin along the c axis gives rise to the spontaneous ferromagnetic moment of about 0.09 μ_B as in $LaMnO_3$, the ferromagnetic component of the Mn^{3+} spin sub-lattice cannot couple to the Pr^{3+} moments because the orientation of the Pr^{3+} ions is along the ab plane, leading to a rather smaller spontaneous ferromagnetic moment along the c axis than in $NdMnO_3$ due to a negligible Pr–Mn exchange interaction.

The specific heats of $PrMnO_3$ near T_N under different magnetic fields up to 8 T are shown in figure 5. It was found that the sharp λ-shaped anomaly under zero field is lowered and broadened by magnetic fields, but the position of the peaks remains unchanged in magnetic fields. Such an effect of magnetic field on the specific heat near the critical point is qualitatively similar to that discussed by Griffiths in the ferromagnet [19]. From the elementary thermodynamic considerations, the specific heat in a magnetic field C_H can be correlated to the temperature dependence of magnetization $M(T, H)$ in terms of

$$(\partial C_H/\partial H)_T = T(\partial^2 M/\partial T^2)_H. \tag{2}$$

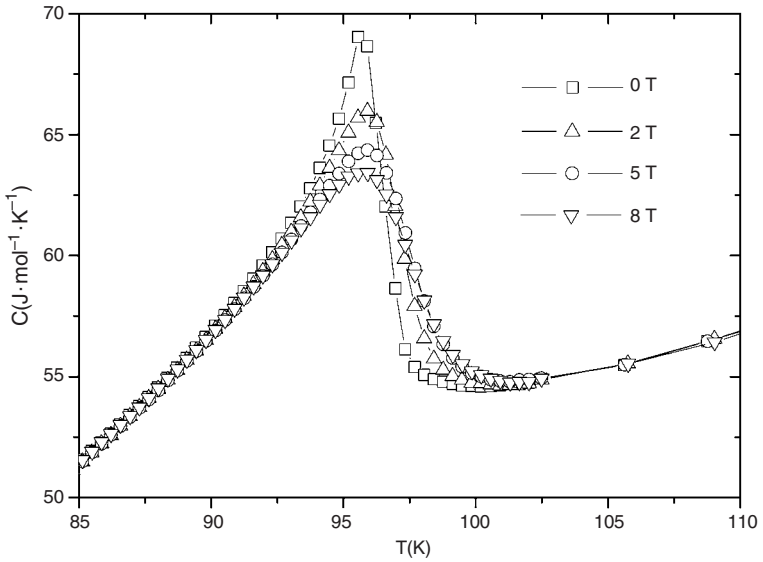

Figure 5. The specific heat of $PrMnO_3$ near T_N under different magnetic fields up to 8 T.

Thus, based on the temperature dependence of magnetization of $PrMnO_3$ in [12], C_H will decrease with H below T_N when the $M(T)$ curve has negative curvature and increase with H above T_N when the curvature of the $M(T)$ curve is positive, with a changeover near T_N. In other words, the increased magnetic energy of the sample by magnetic fields leads to the smooth and broadened behaviour of specific heat near T_N through enhancing the spin fluctuations above T_N by magnetic fields. Such an effect should be reflected in the entropy loss above T_N.

In order to estimate the magnetic entropy near T_N, after subtracting the contribution from the first four singlets of Pr^{3+} ions, the specific heat data above 40 K except those in the region from 50 to 150 K are fitted by using the Thirring model [20, 21]:

$$C_{\mathrm{Lat}} = 3rR\left(1 + \sum_{n=1}^{\infty} B_n u^{-n}\right), \tag{3}$$

where r is number of atoms in the unit cell and R is the ideal-gas constant, $u = [(T/T_b)^2 + 1]$, and $T_b \approx \theta_D/2\pi$. In the case of the Debye solid at temperature $T = \theta_D/4$, equation (3) achieves an accuracy of ~0.03% with only four terms [21]. The above expansion permits the harmonic portion of the lattice specific heat to be fitted reasonably well down to temperatures ~50 K even though the Debye temperature is ~500 K. In our case, we use n up to 4 and the obtained Debye temperatures 440–460 K allow a proper estimation of lattice specific heat down to 40 K with an accuracy of ~0.5%. The fitting parameters as well as the standard deviations under different magnetic fields are summarized in table 2. The resultant magnetic specific heat associated with ordering of Mn spins C_{Mn} under zero field is shown in figure 6. The total magnetic entropy associated with ordering of Mn spins is obtained from numerical integration of C_{Mn}/T from 50 to 150 K, which is also shown in figure 6, as the solid line. It was found that the magnetic entropy due to the ordering of Mn spins is 2.74 J mol^{-1} K^{-1}. Although this value is 48% of the expected $R \ln 2 = 5.76$ J mol^{-1} K^{-1} from an order–disorder transition mainly due to the overestimation of the lattice vibrations, it allows us to evaluate the fraction of entropy loss above T_N (defined as the maximum in the specific heat curves) in the total magnetic entropy denoted as $S(>T_N)/S$. It was found that about 18% of entropy was lost

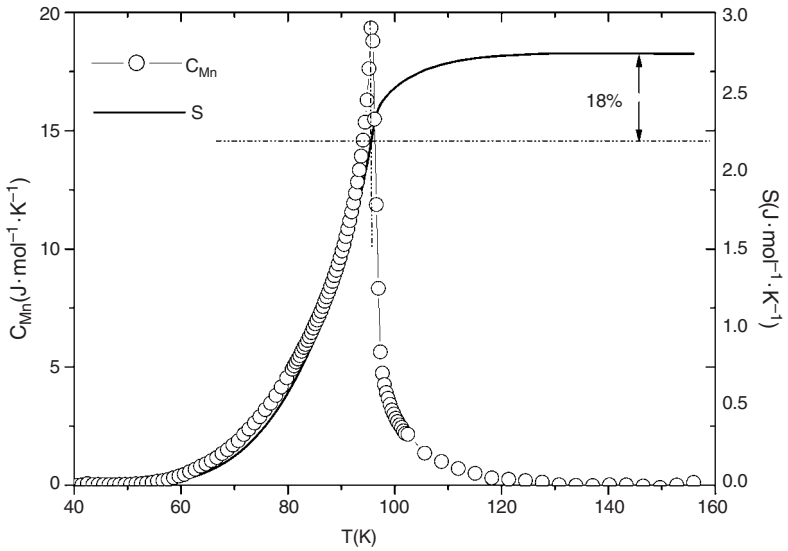

Figure 6. Magnetic specific heat from the Mn^{3+} sub-lattice C_{Mn} near T_N and the magnetic entropy obtained from numerical integration of the C_{Mn}/T in the temperature range.

Table 2. The fit parameters obtained from the high-temperature data under different magnetic fields.

H (T)	0	2	5	8
T_b (K)	73.7(0.8)	71.0(0.5)	70.3(0.7)	70.1(0.6)
B_1	−3.476(0.174)	−3.737(0.187)	−3.756(0.145)	−3.816(0.190)
B_2	7.666(0.281)	8.833(0.252)	8.79(0.240)	9.20(0.256)
B_3	−9.267(0.472)	−11.16(0.540)	−11.0(0.548)	−11.83(0.560)
B_4	4.157(1.208)	5.206(1.270)	5.106(1.256)	5.627(1.279)
$(SD)^2$	0.0513	0.1074	0.1421	0.0932
S (J mol^{-1} K^{-1})	2.74	2.70	2.69	2.67
$S(>T_N)$ (J mol^{-1} K^{-1})	0.50	0.63	0.67	0.71

above T_N under zero field, which arises from the short-range magnetic correlation above T_N. A similar but even more significant effect has been found by Robinson *et al* in the specific heat of antiferromagnetic $NiCl_2{\cdot}6H_2O$ and $CoCl_2{\cdot}6H_2O$ [22], where the fractions of the magnetic entropies gained above T_N were 40% and 52% due to the particularly pronounced short-range order persisting after destruction of the long-range order at T_N. The field dependence of $S(>T_N)/S$ and Debye temperatures derived from the best fit of the high-temperature specific heat data are shown in figure 7. It was found that the $S(>T_N)/S$ increases gradually from 18% under zero field to 27% under 8 T. The magnetic energy induced by magnetic fields enforces the spin fluctuations above T_N gradually with increasing magnetic fields, thus leading to the increase of the entropy loss above T_N. In the $Pr_{0.6}(Ca_{1-x}Sr_x)_{0.4}Mn_3$ system, the entropy loss accompanying the magnetic transition is much smaller than expected, which is partially attributed to the presence of the short-range magnetic correlation above the magnetic ordering temperature [3]. In addition, the Debye temperature under zero field is 463 ± 5 K, which is larger than that derived from low-temperature specific heat [10], but is comparable with the 410 K derived from the high-temperature data in $Pr_{0.63}Ca_{0.37}MnO_3$ [7]. It was found that

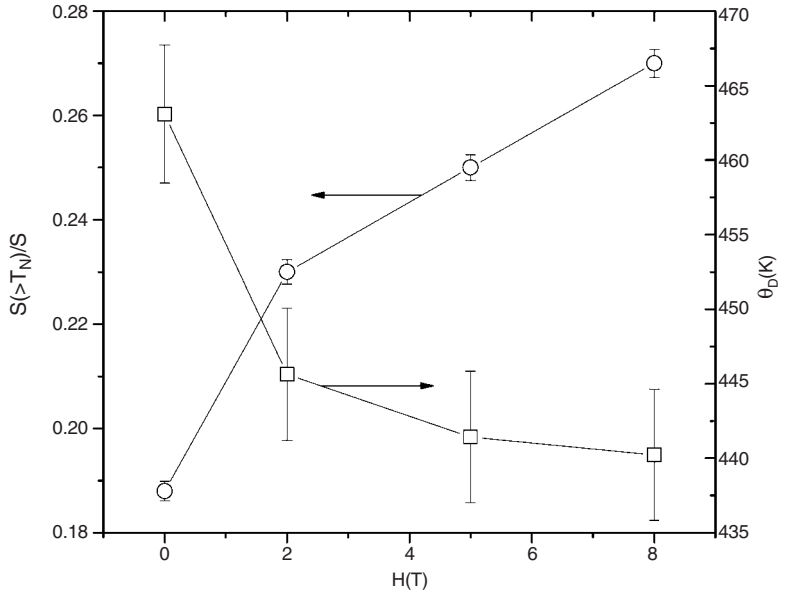

Figure 7. Field dependence of the $S(>T_N)/S$ and Debye temperatures derived from the best fit of the high-temperature specific heat data.

with increasing magnetic fields the Debye temperatures decrease gradually to 440 ± 4 K at $H = 8$ T. Such a decrease of Debye temperatures with magnetic fields is similar to that observed in $NdMnO_3$ and charge-ordered manganites [5, 10], which might be caused by the lattice distortions induced by magnetic field. Recently, Lavrov *et al* described an unexpected magnetic field effect on the crystal shape of an antiferromagnet $La_{2-x}Sr_xCuO_4$ in which the directions of the crystal's axes were swapped and shape changed when the magnetic field was applied [23]. More experiments are necessary to investigate the correlation between the lattice distortions and magnetic field.

4. Conclusion

Specific heat measurements under different magnetic fields up to 8 T were carried out on single-crystal $PrMnO_3$ from 2 to 200 K. A Schottky-like anomaly observed at low temperature was gradually shifted to higher temperatures by magnetic fields. By fitting the specific heat of Pr^{3+} ions below 40 K under zero field, the first four singlets of the Pr^{3+} $^3H_4$ ground multiplet in $PrMnO_3$ are given for the first time to our knowledge. It was found that the absence of the Schottky-like anomaly in the mixed-valent manganites containing Pr^{3+} ions might arise from large splitting of E_1 and E_0 due to their different CEF environments. By analysing the field dependence of E_1 of Pr^{3+} ions, the Pr–Mn exchange field is found to be negligible, which is consistent with the magnetic anisotropy of Pr^{3+} ions revealed in the magnetic measurement. At T_N, the cooperative ordering of Mn^{3+} spins shows up as a λ-shaped anomaly, which is lowered and broadened in magnetic field. It was found that with increasing magnetic field the fraction of entropy above T_N in the total magnetic entropy increases, which originates from the enforced spin fluctuations by magnetic field. In addition, the decrease of the Debye temperature with magnetic field might be caused by the magnetic field-induced structure distortion.

Acknowledgments

We thank Professor J S Zhou at the University of Texas at Austin for providing the crystal and enlightening discussion. This work was supported by the National Natural Science Foundation of China (grant No 10304004) and the Scientific Research Foundation of the Harbin Institute of Technology (grant No HIT.2002.46).

References

[1] Rao C N R and Raveau B 1998 *Colossal Magnetoresistance, Charge Ordering and Related Properties of Manganese Oxides* (Singapore: World Scientific)
[2] Hamilton J J, Keatley E L, Ju H L, Raychaudhuri A K, Smolyaninova V N and Greene R L 1996 *Phys. Rev.* B **54** 14926
[3] Lees M R, Petrenko O A, Balakrishnan G and Paul D Mck 1999 *Phys. Rev.* B **59** 1298
[4] Gordon J E, Fisher R A, Jia Y X, Phillips N E, Reklis S F, Wright D A and Zettl A 1999 *Phys. Rev.* B **59** 127
[5] López J, de Lima O F, Lisboa-Filho P N and Araujo-Moreira F M 2002 *Phys. Rev.* B **66** 214402
[6] Smolyaninova V N, Amlan B, Zhang X, Kim K H, Kim B-G, Cheong S W and Greene R L 2000 *Phys. Rev.* B **62** R6093
[7] Raychaudhuri A K, Ayan G, Das I, Rawat R and Rao C N R 2001 *Phys. Rev.* B **64** 165111
[8] Hardy V, Wahl A, Martin C and Simon Ch 2001 *Phys. Rev.* B **63** 224403
[9] Hemberger J, Brando M, When R, Ivanv V Yu, Mukhin A A, Balbashov A M and Loidl A 2004 *Phys. Rev.* B **69** 064418
[10] Cheng J G, Sui Y, Qian Z N, Liu Z G, Miao J P, Huang X Q, Lu Z, Li Y, Wang X J and Su W H 2005 *Solid State Commun.* **134** 381
[11] Ashcroft N W and Mermin N D 1975 *Solid State Physics* (Philadelphia, PA: Saunders)
[12] Mukhin A A, Ivanov V Yu, Travkin V D and Balbashov A M 1999 *J. Magn. Magn. Mater.* **226** 1139
[13] Zhou J S and Goodenough J B 2003 *Phys. Rev.* B **68** 054403
[14] Zhou J S and Goodenough J B 2003 *Phys. Rev.* B **68** 144406
[15] Bartolomé F, Bartolomé J, Castro M and Melero J J 2000 *Phys. Rev.* B **62** 1058
[16] Rosenkranz S, Medarde M, Fauth F, Mesot J, Zolliker M, Furrer A, Staub U, Lacorre R, Osborn R, Eccleston R S and Trounov V 1999 *Phys. Rev.* B **60** 14857
[17] Podlesnyak A, Rosenkranz S, Fauth F, Marti W, Scheel H J and Furrer A 1994 *J. Phys.: Condens. Matter* **6** 4099
[18] Kittel C 1976 *Introduction to the Solid State Physics* 5th edn (New York: Wiley)
[19] Griffiths R B 1969 *Phys. Rev.* **188** 942
[20] Thirring H 1913 *Z. Phys.* **14** 867
[21] Gordon J E, Tan M L, Fisher R A and Phillips N E 1989 *Solid State Commun.* **69** 625
[22] Robinson W K and Friedberg S A 1960 *Phys. Rev.* **117** 402
[23] Lavrov A N, Komiya S and Ando Y 2002 *Nature* **418** 385